Characterization of biotin-anandamide, a novel tool for the visualization of anandamide accumulation

Filomena Fezza,[1,*,†] Sergio Oddi,[1,*,§] Monia Di Tommaso,[†,§] Chiara De Simone,[*,†] Cinzia Rapino,[§] Nicoletta Pasquariello,[§] Enrico Dainese,[§] Alessandro Finazzi-Agrò,[†] and Mauro Maccarrone[2,*,§]

European Center for Brain Research/Istituto di Ricovero e Cura a Carattere Scientifico S. Lucia Foundation,[*] Rome, Italy; Department of Experimental Medicine and Biochemical Sciences,[†] University of Rome Tor Vergata, Rome, Italy; and Department of Biomedical Sciences,[§] University of Teramo, Teramo, Italy

Abstract Anandamide (*N*-arachidonoylethanolamide; AEA) acts as an endogenous agonist of both cannabinoid and vanilloid receptors. During the last two decades, its metabolic pathways and biological activity have been investigated extensively and relatively well characterized. In contrast, at present, the effective nature and mechanism of AEA transport remain controversial and still unsolved issues. Here, we report the characterization of a biotinylated analog of AEA (b-AEA) that has the same lipophilicity of the parent compound. In addition, by means of biochemical assays and fluorescence microscopy, we show that b-AEA is accumulated inside the cells in a way superimposable on that of AEA. Conversely, b-AEA does not interact or interfere with the other components of the endocannabinoid system, such as type-1 and type-2 cannabinoid receptors, vanilloid receptor, AEA synthetase (*N*-acylphosphatidylethanolamine-hydrolyzing phospholipase D), or AEA hydrolase (fatty acid amide hydrolase). ▮▮ Together, our data suggest that b-AEA could be a very useful probe for visualizing the accumulation and intracellular distribution of this endocannabinoid.—Fezza, F., S. Oddi, M. Di Tommaso, C. De Simone, C. Rapino, N. Pasquariello, E. Dainese, A. Finazzi-Agrò, and M. Maccarrone. **Characterization of biotin-anandamide, a novel tool for the visualization of anandamide accumulation.** *J. Lipid Res.* 2008. **49:** 1216–1223.

Anandamide (*N*-arachidonoylethanolamine; AEA) is an endogenous agonist of type-1 (CB1R) and type-2 (CB2R) cannabinoid receptors (1–3) CB1R is localized mainly in the central nervous system (4) but is also expressed in peripheral districts like immune cells (5–7); conversely, CB2R is expressed predominantly in the periphery but is also present in the brain (8, 9). Therefore, the activation of CB1 or CB2 receptors by AEA has many central (10) and peripheral (11) effects, which are terminated by cellular uptake (12–14), followed by degradation to ethanolamine and arachidonic acid (AA) by the fatty acid amide hydrolase (FAAH) (15). AEA is biosynthesized mainly by a specific *N*-acylphosphatidylethanolamine-hydrolyzing phospholipase D (NAPE-PLD), which releases "on demand" AEA from membrane NAPEs (16, 17). In addition, other biosynthetic pathways of AEA have been discovered recently (18–20). Together with AEA and other congeners, like 2-arachidonoylglycerol, *N*-arachidonoyldopamine, noladin ether, and virodhamine, the proteins that bind, transport, synthesize, and hydrolyze these lipids form the "endocannabinoid system" (21, 22). Also, the ability of AEA to bind to and activate type-1 vanilloid receptors [now called transient receptor potential channel vanilloid receptor subunit 1 (TRPV1)] has attracted growing interest (23). For instance, the activation of CB1R or TRPV1 by AEA can exert opposite biological effects, like protection against or induction of apoptosis in neuronal and peripheral cells (24, 25), respectively.

A still unresolved, although critical, issue in endocannabinoid research is the mechanism by which AEA crosses the plasma membrane and is transported inside the cells (12–14, 26). Because the intracellular accumulation of AEA is known to be temperature-dependent, saturable, substrate-specific, and subjected to specific inhibition by AA derivatives, the existence of a selective AEA membrane transporter has been postulated (27, 28). However, the molecular identity of the purported transporter remains unknown, and at present molecular probes to test its expression at the protein or mRNA level are not available. In addition, the kinetic features of AEA uptake do not rule out other mechanisms of transmembrane transport, being compatible, for example, with a simple diffusion process driven by FAAH-catalyzed hydrolysis of AEA. In this line, whether and to what extent FAAH activity may control the uptake of AEA is still unclear,

[1] F. Fezza and S. Oddi contributed equally to this study.
[2] To whom correspondence should be addressed.
e-mail: mmaccarrone@unite.it

although pharmacological (29, 30), biochemical (31, 32), and immunofluorescence microscopy (32) studies strongly suggest that an authentic AEA membrane transporter may exist and it may be distinct from FAAH. To shed some light on the degradation pathway of AEA, which is critical for the metabolic control of its biological activity (33–35), it would be very important to visualize by means of microscopy techniques the accumulation and intracellular distribution of AEA. However, analogs of AEA or other molecular tools designed to this end are not yet available. The aim of the present investigation was to characterize a biotinylated analog of AEA (b-AEA or MM22) designed to visualize the intracellular accumulation of this endocannabinoid through immunomicroscopy techniques. We chose to modify the polar head of AEA because this structural change does not influence the kinetics of AEA uptake, as reported (21).

In the present study, we used the human keratinocytes (HaCaT cells), because they have a full and functional endocannabinoid system (36) and are suitable for immunomicroscopy studies (32). By means of biochemical assays and morphological analysis, here we show that biotinylation of the polar head of AEA does not affect its accumulation by the cells but prevents its interaction with FAAH, NAPE-PLD, CB1R, CB2R, and TRPV1.

MATERIALS AND METHODS

Materials

Chemicals were of the purest analytical grade. [³H]AEA (205 Ci/mmol), [³H]AA (98.60 Ci/mmol), [³H]CP55.940 (126 Ci/mmol), and [³H]resinferatoxin ([³H]RTX; 43 Ci/mmol) were from Perkin-Elmer Life Sciences, Inc. (Boston, MA). [³H]N-Arachidonoylphosphatidylethanolamine ([³H]NArPE; 200 Ci/mmol) was from American Radiolabeled Chemicals (St. Louis, MO). AEA, AA, and 12-O-tetradecanoylphorbol 13-acetate were from Sigma Chemical Co. (St. Louis, MO). Cyclohexylcarbamic acid 3′-carbamoyl-biphenyl-3-yl ester (URB597) and (S)-1′-(4-hydroxybenzyl)-oleoyl-ethanolamide (OMDM-1) were from Cayman Chemical (Ann Arbor, MI), and capsazepine was from Calbiochem (La Jolla, CA). EZ-Link Biotin-PEO-Amine was from Pierce (Rockford, IL). N-Piperidino-5-(4-chlorophenyl)-1-(2,4-dichloro-phenyl)-4-methyl-3-pyrazole carboxamide (SR141716) and N-[1(S)-endo-1, 3,3-trimethyl-bicyclo [2.2.1]heptan-2-yl]5-(4-chloro-3-methylphenyl)-1-(4-methyl-benzyl)-pyrazole-3-carboxa-mide (SR144528) were kind gifts from Sanofi-Aventis Recherche (Montpellier, France). Unlabeled NArPE was synthesized from AA and phosphatidylethanolamine as reported (17). Anti-CB1R and anti-CB2R rabbit polyclonal antibodies were purchased from Cayman Chemical. Mouse anti-biotin antibody, anti-mouse conjugated to Alexa Fluor 488, or anti-rabbit conjugated to horseradish peroxidase secondary antibodies and the Prolong antifade kit were purchased from Molecular Probes (Eugene, OR).

Synthesis of b-AEA

We prepared b-AEA (**Fig. 1A**) using the EZ-Link Biotin-PEO-Amine. Briefly, the AA was activated using an amide-coupling reagent and then treated with the biotin tag in basic medium (37). The synthesis of the radiolabeled [³H]b-AEA was carried out under the same experimental conditions using a mix of AA and [³H]AA (specific activity, 10 mCi/mmol).

Assay of AEA and b-AEA metabolism in HaCaT cells

The activity of AEA uptake was studied in intact HaCaT cells, as described (36). Cells were incubated for 10 min at 37°C with [³H]AEA or [³H]b-AEA as substrate and washed three times in 1 ml of PBS containing 1% BSA; then, they were resuspended in 0.5 ml (0.5 M) of NaOH and measured in a scintillation
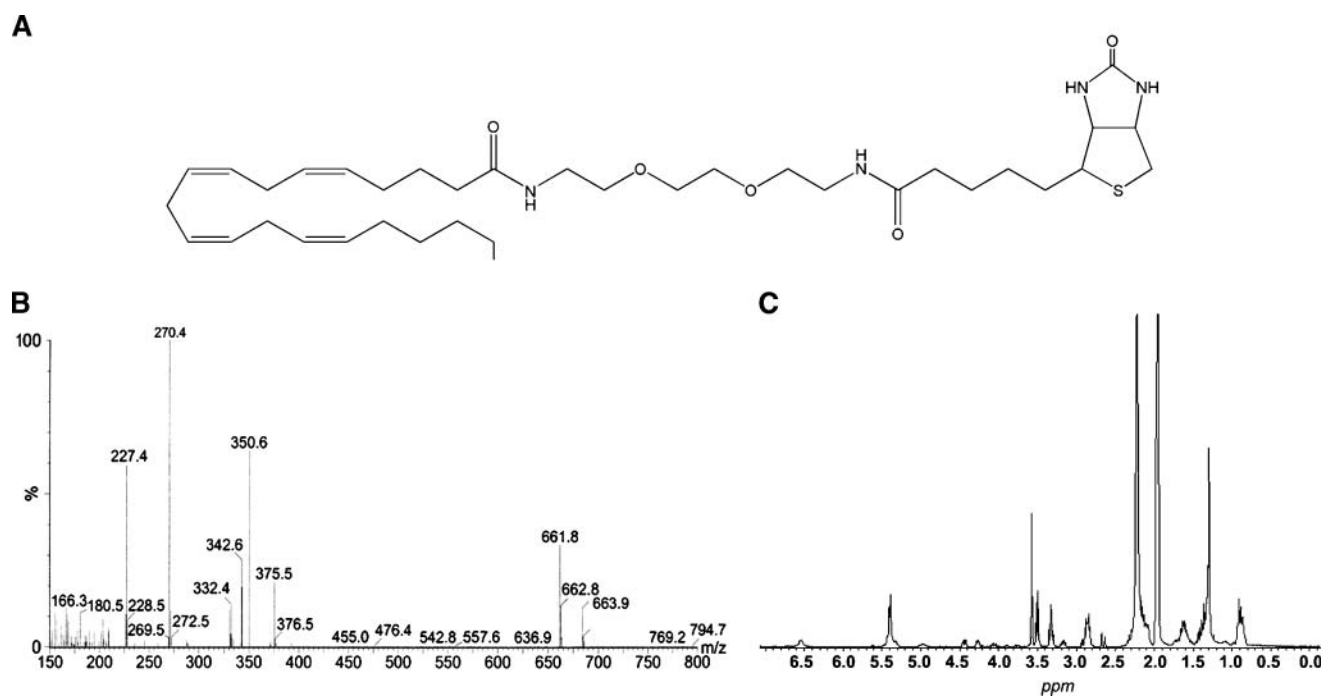

Fig. 1. Chemical structure (A), MS spectrum (B), and ¹H NMR spectrum (C) of the biotinylated analog of N-arachidonoylethanolamine (b-AEA).

counter. To further discern non-carrier-mediated from carrier-mediated transport of [³H]AEA or [³H]b-AEA across cell membranes, control experiments were carried out at 4°C. The effect of different compounds on [³H]AEA or [³H]b-AEA uptake was determined by adding each substance directly to the incubation medium at the indicated concentrations (36).

FAAH activity was assayed in HaCaT cell extracts (100 μg/test) by measuring the release of [³H]AA from [³H]AEA or [³H]b-AEA through reverse-phase (RP)-HPLC (38). Also, the effect of cold b-AEA on the hydrolysis of [³H]AEA was ascertained by adding the biotin derivative directly to the assay buffer.

NAPE-PLD activity was assayed in HaCaT cell extracts (100 μg/test) by measuring the release of [³H]AEA from [³H]NArPE (100 μM) through RP-HPLC (17). The effect of b-AEA on NAPE-PLD activity was ascertained by adding the biotin derivative directly to the assay buffer.

Both AEA uptake and FAAH activity data were elaborated through nonlinear regression analysis using the Prism 4 program (GraphPAD Software for Science, San Diego, CA) to calculate apparent K_m and V_{max} of [³H]AEA or [³H]b-AEA. Concentrations of b-AEA able to reduce by half (IC_{50}) the uptake, hydrolysis, and synthesis of AEA through uptake, FAAH activity, and NAPE-PLD activity, respectively, were calculated from dose-response curves drawn with b-AEA concentrations up to 10 μM.

Receptor binding assays

For cannabinoid receptor studies, HaCaT cells, mouse brain, or mouse spleen were homogenized in 2 mM Tris-EDTA, 320 mM sucrose, 5 mM MgCl₂, and 100 μM PMSF buffer (pH 7.4) using a Potter homogenizer and were centrifuged three times at 1,000 g (10 min), discharging the pellet. The supernatant was centrifuged at 18,000 g (30 min), and the pellet was resuspended in assay buffer (50 mM Tris-HCl, 2 mM Tris-EDTA, 3 mM MgCl₂, and 100 μM PMSF, pH 7.4) to a final protein concentration of 1 mg/ml. These membrane fractions were used in rapid filtration assays with [³H]AEA, [³H]b-AEA, or [³H]CP55.940 (36). For the assay of vanilloid receptors, which are not expressed by HaCaT cells (36), membrane fractions isolated from rat neuroblastoma C6 cells were used in rapid filtration assays with [³H]RTX as reported (39). The effects of different compounds on CBR or TRPV1 binding were tested as reported (36, 39). Binding data from HaCaT cells and mouse brain membranes were elaborated through nonlinear regression analysis, using the Prism 4 program, to calculate apparent dissociation constant (K_d) and maximum binding (B_{max}) of [³H]AEA, [³H]b-AEA, or [³H]CP55.940. IC_{50} values of b-AEA toward the binding of [³H]CP55.940 to CBRs and of [³H]RTX to TRPV1 were calculated from dose-response curves.

Western blot analysis

Western blotting was performed according to standard procedures (36). The following antibodies were used to immunodetect CB1 and CB2 receptors: anti-CB1R and anti-CB2R rabbit polyclonal antibodies.

Fluorescence microscopy studies in HaCaT cells

HaCaT cells were grown on collagen-coated glass coverslips and were incubated either with 5 μM biotin tag (as a negative control) or with 5 μM b-AEA for 10 min at 37°C. The effects of 5 μM OMDM-1, a selective inhibitor of AEA transport (29), of 0.1 μM URB597, a selective inhibitor of the AEA hydrolase FAAH (40), and of 0.5 μM SR141716 or 0.5 μM SR144528, CB1 or CB2 receptor-selective antagonists, respectively (41), on the uptake of b-AEA were determined by adding each substance

directly to the incubation medium at 5 min before b-AEA addition. Cells were washed, fixed with 4% paraformaldehyde for 30 min at room temperature, and then permeabilized with 0.1% Triton X-100 in PBS for 2 min at 4°C. After a blocking step in 5% BSA in PBS for 30 min at room temperature, cells were incubated for 1 h at room temperature with anti-biotin primary antibody diluted 1:100 in blocking solution. Anti-mouse secondary antibodies conjugated to Alexa Fluor 488 were diluted 1:200 in blocking solution and incubated with the specimens for 30 min at room temperature. After washing, the coverslips were mounted using an antifade reagent and visualized with a Nikon Eclipse E800 fluorescence microscope equipped with a filter pack for green fluorescence detection (excitation wavelength = 465–495, emission wavelength = 515–555) (Nikon Instruments, Tokyo, Japan). For image analysis, five fields from at least three independent experiments were examined for each treatment. Quantification of the mean fluorescence intensity in selected regions was carried out using ImageJ software http://rsb.info.nih.gov/ij/).

Statistical analysis

Data reported in this paper are means ± SD of at least three independent experiments, each performed in duplicate. Statistical analysis was performed by the nonparametric Mann-Whitney U-test, elaborating experimental data by means of the InStat 3 program (GraphPAD Software for Science).

RESULTS

Characterization of b-AEA

Previous studies have indicated that the kinetic parameters of AEA uptake are sensitive to modification of the arachidonate moiety, whereas changes in the ethanolamide region are well tolerated (42, 43). Therefore, we designed b-AEA, in which the biotin tag was attached to the polar head of AEA through a spacer arm (Fig. 1A).

The synthetic route of b-AEA allowed us to produce both b-AEA and its tritium-labeled analog ([³H]b-AEA) with a yield of ∼50%. The identity and purity of b-AEA was checked by HPLC-ESI-MS and by ¹H NMR. HPLC-ESI-MS was performed with a Waters apparatus (Milford, MA), and ¹H NMR was recorded on a Bruker AM series spectrometer (Rheinstetten, Germany) at 300 K and 300 MHz. Biotin-AEA showed an MS spectrum (Fig. 1B) with m/z = 661.8 [M+H]⁺ and a ¹H NMR (CD3CN) spectrum (Fig. 1C) with δ: 0.88 (3H, t, J = 5.1 Hz), 1.24–1.47 (6H, m), 1.49–1.74 (8H, m), 2.06–2.31 (8H, m, partially under water residual peak), 2.66 (1H, d, J = 12.9 Hz), 2.77–2.96 (7H, m), 3.14–3.23 (1H, m), 3.26–3.36 (4H, m), 3.46–3.55 (4H, m), 3.58 (4H, s), 4.18–4.29 (1H, m), 4.40–4.46 (1H, m), 5.26–5.48 (8H, m), 6.51–6.56 (bs, 2H).

Interestingly, the addition of the biotin tag did not yield any major change in lipophilicity, expressed as logarithm of the partition coefficient in n-octanol/water (LogP in **Fig. 2**), calculated through the HyperChem™ 6.03 Molecular Modeling System (Hypercube, Inc., Gainesville, FL). Also, the analysis of low-energy conformations of AEA and b-AEA showed similar electrostatic potentials on the acyl chain moiety (Fig. 2). These conformations were obtained using molecular mechanics geometry optimization

Compound	Molecular Weight	Logarithm of Partition Coefficient [n-Octanol/Water] (LogP)
AEA	347.53	5.1
b-AEA	660.95	4.7
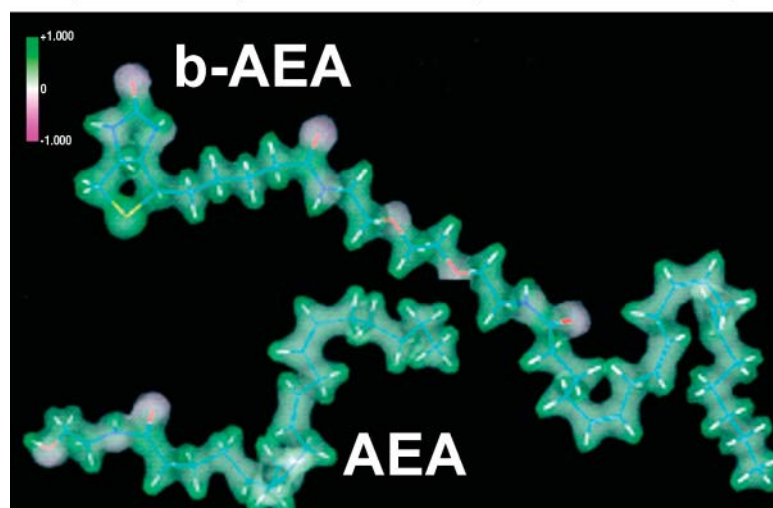
Fig. 2. Molecular properties of AEA versus b-AEA. The molecular weight, lipophilicity (LogP), and electrostatic potential of AEA are compared with those of b-AEA. Low-energy conformations of AEA and b-AEA are reported in the bottom panel and show the electrostatic potential on the molecular surface (violet, −1; green, +1).

with the AMBER94 force field, followed by single-point calculations (HyperChem™ 6.03), as reported (44).
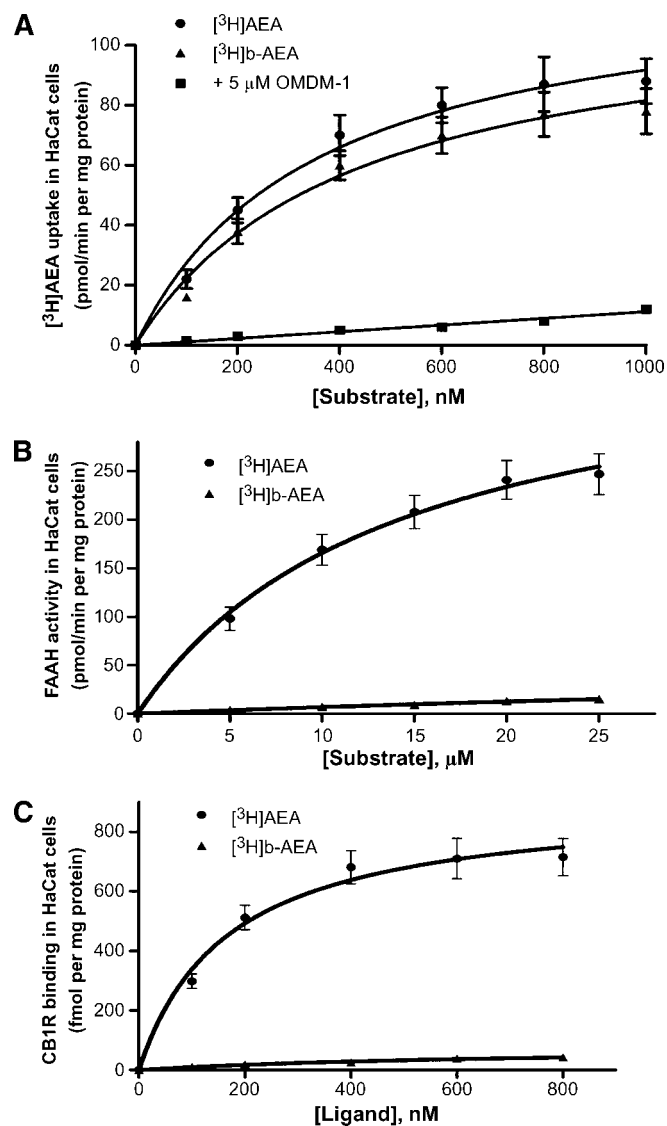
Metabolism of AEA and b-AEA in HaCaT cells

Intact HaCaT cells were able to accumulate [³H]b-AEA in a concentration-dependent manner, typical of a saturable process (**Fig. 3A**). Accumulation of [³H]b-AEA was similar to that of [³H]AEA (Fig. 3A) and showed apparent K_m and V_{max} values of 421 ± 88 nM and 116 ± 10 pmol/min/mg protein, respectively (**Table 1**). These kinetic constants are typical of AEA transport in HaCaT cells (36) as well as in other cell types (12–14). In addition, 5 µM OMDM-1, a selective AEA uptake inhibitor (29), minimized the uptake of [³H]b-AEA (Fig. 3A) in much the same way as it inhibited that of [³H]AEA in the same cells (data not shown) (32). Unlike [³H]AEA, which was hydrolyzed in a concentration-dependent manner (Fig. 3B) and with kinetic constants (Table 1) typical of FAAH in HaCaT cells (36), [³H]b-AEA was not a substrate for FAAH (Fig. 3B). In particular, we found only intact [³H]b-AEA when we analyzed by RP-HPLC the organic extract of the enzymatic reaction, demonstrating that b-AEA is metabolically stable (data not shown). Furthermore, [³H]b-AEA did not bind to CB1R of HaCaT cells (Fig. 3C), at variance with [³H]AEA, which bound to these receptors (Fig. 3C) with apparent K_d and B_{max} values (Table 1) close to those already found in HaCaT cells (36). Likewise, SR141716 (0.5 µM), but not SR144528 (0.5 µM), which are selective antagonists of CB1 or CB2 receptors, respectively (2, 41), reduced the binding of 400 nM [³H]AEA to HaCaT cell membranes to ~15% of control values, corroborating previous data (36).

To further characterize the biochemical profile of biotin-AEA, we performed inhibition assays aimed at calculating the concentration of b-AEA able to reduce by half (IC$_{50}$)

the transport, hydrolysis, and biosynthesis of [³H]AEA. The results, shown in **Table 2**, demonstrate that b-AEA does not affect FAAH activity or NAPE-PLD activity of HaCaT cells when used at concentrations up to 10 µM; yet, it does reduce the uptake of 0.5 µM AEA, with an IC$_{50}$ value of 0.5 ± 0.1 µM, indicating very similar affinities of the transport machinery toward AEA and its biotinylated derivative (Table 2).

We also tested the ability of b-AEA to inhibit the binding of [³H]CP55.940, a synthetic agonist of CBRs. To this end, membrane preparations from mouse brain or mouse spleen were used as sources of authentic type-1 and type-2 CB receptors, respectively [2, 41]. As expected, we detected by Western blot immunoreactivity for CB1R in the mouse whole brain and for CB2R in the spleen; conversely, we did not observe any immunoreactivity for CB1R in the spleen and for CB2R in the brain (data not shown). Likewise, we also investigated the ability of b-AEA to bind to TRPV1 by performing competition assays with the specific receptor agonist [³H]RTX (23, 45). The results, summarized in Table 2, demonstrate that b-AEA was inactive toward CB2 or TRPV1 receptors at concentrations up to 10 µM, whereas it was able to inhibit by 50% CB1R binding at 5 ± 0.7 µM (Table 2). To further analyze the interaction of b-AEA with CB1R, we calculated the K_d and B_{max} values for CP55.940 (concentration range, 0–1 nM) in the absence or presence of 10 µM b-AEA. We found that b-AEA did not affect K_d (720 ± 100 vs. 734 ± 110 pM of controls) but reduced B_{max} almost by half (517 ± 72 vs. $1,150 \pm 200$ fmol/mg protein of controls).

Together, the biochemical data suggest that b-AEA is not a substrate for FAAH, does not interfere with NAPE-PLD, and is not efficiently recognized by the AEA binding receptors; however, b-AEA is transported by the same machinery, and with the same efficiency, as AEA.

Fig. 3. Metabolism of AEA versus b-AEA in HaCaT cells. A: Transport of [^{3}H]AEA and [^{3}H]b-AEA alone. The effect of 5 μM (*S*)-1′-(4-hydroxybenzyl)-oleoylethanolamide (OMDM-1) refers to the uptake of [^{3}H]b-AEA and was superimposable on the effect on the uptake of [^{3}H]AEA (omitted for the sake of clarity). B: Hydrolysis by fatty acid amide hydrolase (FAAH). C: CB1R binding. Error bars represent SD values.

Immunofluorescence studies of b-AEA accumulation

To ascertain whether b-AEA can be used as a probe to visualize the internalization of AEA by intact cells, we next performed immunofluorescence microscopy studies in human HaCaT keratinocytes. b-AEA was detected by indirect immunofluorescence using an anti-biotin monoclonal antibody and an anti-mouse secondary antibody conjugated with a green fluorescent dye. The immunostaining revealed that cells quickly (within 5 min) took up b-AEA, which appeared to accumulate both in the cytosol and in the nucleus (**Fig. 4**, b-AEA). Interestingly, the biotin tag per se was not taken up by the cells under the same experimental conditions (Fig. 4, Ctrl).

TABLE 1. Kinetic constants of AEA uptake, FAAH activity, or CB1R binding in HaCaT cells using AEA or b-AEA as substrate or ligand

Parameter		Kinetic Constant
AEA uptake	K_m (nM)	V_{max} (pmol/min/mg protein)
AEA	353 ± 60	124 ± 8
b-AEA	421 ± 88	116 ± 10
FAAH	K_m (μM)	V_{max} (pmol/min/mg protein)
AEA	13 ± 2	385 ± 25
b-AEA	——	——
CB1R	Dissociation constant (nM)	Maximum binding (fmol/mg protein)
AEA	173 ± 38	926 ± 63
b-AEA	——	——

AEA, *N*-arachidonoylethanolamine; b-AEA, biotinylated analog of AEA; FAAH, fatty acid amide hydrolase.

In addition, we tested the specificity of b-AEA immunostaining in the presence of 5 μM OMDM-1 or 0.1 μM URB597. A remarkable decrease in immunostaining was observed only in HaCaT cells pretreated with OMDM-1, strongly indicating that b-AEA was indeed taken up by a transporter-dependent process (Fig. 4). Instead, the inhibition of FAAH activity by 0.1 μM URB597 did not affect the intracellular accumulation of b-AEA, nor did 0.5 μM SR144528 (Fig. 4) or 10 μM capsazepine, a selective antagonist of TRPV1 (data not shown) (23, 45). On the other hand, 0.5 μM SR141716 was able to decrease the fluorescence intensity by ∼35% of the control (Fig. 4), indicating a contribution of CB1R to AEA uptake (32, 46, 47).

DISCUSSION

In this investigation, we report the characterization of a biotinylated derivative of anandamide and show through

TABLE 2. IC$_{50}$ values of b-AEA toward uptake, hydrolysis, and biosynthesis of AEA and toward CB1R, CB2R, and TRPV1 binding

Parameter	IC$_{50}$
	μM
Uptake[a]	0.5 ± 0.1
FAAH[b]	>10
NAPE-PLD[c]	>10
CB1R[d]	5 ± 0.7
CB2R[e]	>10
TRPV1[f]	>10

NAPE-PLD, *N*-acylphosphatidylethanolamine-hydrolyzing phospholipase D; TRPV1, transient receptor potential channel vanilloid receptor subunit 1. Data are means ± SD of three independent experiments.
[a] Uptake was measured in intact HaCaT cells with 400 nM [^{3}H] AEA as substrate (control = 80 ± 9 pmol/min/mg protein).
[b] Activity was measured in HaCaT cell extracts with 10 μM [^{3}H] AEA as substrate (control = 170 ± 18 pmol/min/mg protein).
[c] Activity was measured in HaCaT cell extracts with 100 μM [^{3}H] *N*-arachidonoylphosphatidylethanolamine as substrate (control = 12 ± 3 pmol/min/mg protein).
[d] Binding was measured in mouse brain membrane fractions with 400 pM [^{3}H]CP55.940 as ligand (control = 82 ± 8 fmol/mg protein).
[e] Binding was measured in mouse spleen membrane fractions with 400 pM [^{3}H]CP55.940 as ligand (control = 58 ± 4 fmol/mg protein).
[f] Binding was measured in C6 cell membrane fractions with 500 pM [^{3}H]resinferatoxin as ligand (control = 141 ± 22 fmol/mg protein).
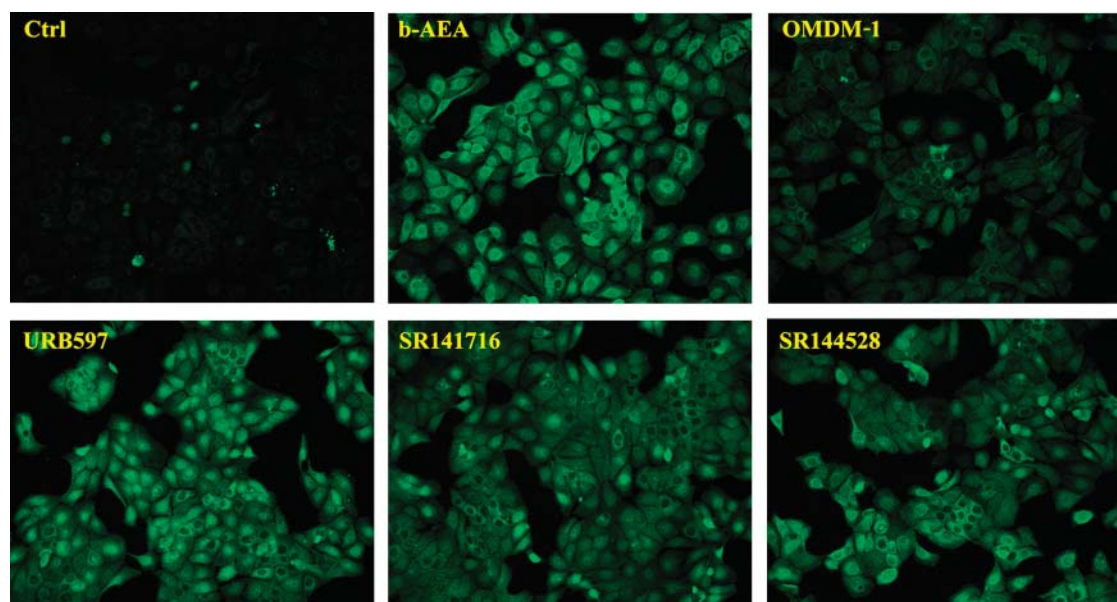
	Ctrl	b-AEA (5 µM)	b-AEA + OMDM-1 (5 µM)	b-AEA + URB597 (0.1 µM)	b-AEA + SR141716 (0.5 µM)	b-AEA + SR144528 (0.5 µM)
Fluorescence Intensity (AU)	13 ± 2	98 ± 10	37 ± 5*	90 ± 8	64 ± 7**	82 ± 10

* p<0.01 vs b-AEA
**p<0.05 vs b-AEA

Fig. 4. Fluorescence microscopy studies of the distribution of b-AEA in HaCaT cells. No green fluorescence could be detected in negative controls, demonstrating that the biotin tag was not able per se to cross the plasma membrane (Ctrl). Instead, 5 µM b-AEA was internalized, and this process was minimized by 5 µM OMDM-1 and partly by 0.5 µM *N*-piperidino-5-(4-chlorophenyl)-1-(2,4-dichloro-phenyl)-4-methyl-3-pyrazole carboxamide (SR141716), but not by 0.1 µM cyclohexylcarbamic acid 3′-carbamoyl-biphenyl-3-yl ester (URB597) or 0.5 µM *N*-[1(*S*)-endo-1,3,3-trimethyl-bicyclo [2.2.1]heptan-2-yl]5-(4-chloro-3-methylphenyl)-1-(4-methyl-benzyl)-pyrazole-3-carboxa-mide (SR144528). Images are representative of at least three independent experiments, and five fields were examined for each treatment. Fluorescence intensity (AU, arbitrary units) was quantified by ImageJ software, and values represent means ± SD.

biochemical, morphological, and functional assays that b-AEA is a suitable tool to visualize the accumulation of this endocannabinoid in intact cells.

In the last few years, the biosynthesis and degradation of AEA have been clarified in considerable detail, leading to the molecular cloning and characterization of the AEA hydrolase FAAH (15) and of the AEA synthetase NAPE-PLD (16). To be metabolized by FAAH, AEA must be transported across the plasma membrane to the intracellular compartments where FAAH is localized (32). Yet, the mechanism of AEA uptake has remained elusive, and to date a general consensus has been reached only on the fact that AEA movement through the plasma membrane is rapid, saturable, temperature-dependent, and energy (supplied as ATP or ion gradients)-independent (12–14). Against >100 papers describing a transporter-mediated uptake of AEA via a selective "anandamide membrane transporter," a few papers recently proposed that the transport occurs by simple diffusion or endocytosis via caveolae/lipid rafts (13, 48). As a matter of fact, the lack of cloning and expression of the purported transporter protein has prevented the development of molecular tools like oligonucleotides or antibodies, which are able to give definitive proof of the presence of a true transporter on the cell surface. In the same line, AEA analogs able to visual-ize AEA movement across the plasma membrane, and its subsequent fate within the cell, are still missing.

To date, besides radiolabeled AEA, only two other compounds have been developed to investigate these aspects of AEA metabolism. The first compound is a fluorescein isothiocyanate-conjugated analog of AEA named SKM 4-45-1 (42). This substance becomes fluorescent upon hydrolysis by cytosolic esterases, releasing the fluorescein moiety. Therefore, its use should be restricted to cells that express enough esterase activity (42) and is not suitable to visualize AEA adsorption on the cell surface (32). Another critical limitation of SKM 4-45-1 is that the appearance of intracellular fluorescence depends on two kinetic processes (i.e., uptake and intracellular hydrolysis). Therefore, the suitability of SKM 4-45-1 for kinetic studies of AEA transport is rather limited. Furthermore, because of the low degree of signal associated with direct fluorescence, SKM 4-45-1 did not prove to be of particular efficacy for fine morphological analysis of AEA accumulation and metabolism (42, 48). The second compound, LY2318912, has been described as a potent, competitive inhibitor of AEA uptake that has made it possible to identify a high-affinity binding site specifically involved in the transport of this endocannabinoid (49). However, the selectivity of LY2318912 has been questioned recently,

because one of its congeners, LY2183240, turned out to be also a potent inhibitor of FAAH (50, 51). Against this background, the biotinyl derivative of AEA described here seems to be a unique tool for the visualization of AEA accumulation by fluorescence microscopy techniques, which are safer, cheaper, and easier to use than radiographic methods. In particular, the widespread use of biotin as a target for antibody recognition seems to warrant the wide exploitation of b-AEA in several immunological applications, including the imaging of AEA transport and distribution in various cell types.

We chose to modify the polar head of AEA because previous studies indicated that the kinetics of AEA uptake is sensitive to the modification of the arachidonate moiety, whereas changes in the ethanolamide region are ineffective (21, 42). On the other hand, analogs with bulky groups on the polar head have been shown to exhibit poor affinity for both CB1 and CB2 receptors and almost no activity for TRPV1 receptors and for FAAH (43). It seems noteworthy that the biochemical profile of b-AEA shows that it is well recognized only by mechanisms responsible for AEA transport but not by other elements of the endocannabinoid system. Accordingly, the biotin derivative of AEA contains the four *cis* nonconjugated double bond motifs that lead to the U-shaped conformation fundamental for the interaction with the transport machinery (21). On the other hand, the hydroxyl group of AEA, considered important for the interaction with FAAH (21), is not available in b-AEA because it is derivatized with the biotin tag. Regarding the possible interaction between b-AEA and CB1R, we found that b-AEA interacts with CB1R moderately and only at micromolar concentrations. Further assays aimed at determining the effect of b-AEA on the binding constants for CP55.940 demonstrated that b-AEA does not affect K_d but reduces B_{max} almost by half. By analogy with enzyme kinetics, these findings demonstrate that b-AEA does not bind to the ligand binding site of the receptor but rather interferes with CB1R by some other "noncompetitive" mechanism(s).

Another important issue concerns the possible role of CB1R on AEA uptake; in this context, we found that the blockade of CB1R with SR141716 significantly reduced b-AEA uptake. In keeping with previous studies from our (32, 46) and other (47) laboratories, showing that AEA transport is partly inhibited (by ∼20%) by SR141716, this result supports the notion that CB1R is somehow involved in the internalization of AEA and that the cellular uptake of AEA is a complex process that involves multiple proteins.

Together, these observations might open the avenue to new structure-activity relationship studies aimed at elucidating the molecular determinants that confer to b-AEA specificity over AEA itself. In agreement with this, it should be recalled that the transporter-mediated movement across the plasma membrane is a key step in regulating the biological activity of AEA, both centrally and peripherally, and is considered a major target for drug development (21, 52).

In conclusion, we report unprecedented evidence that b-AEA is a suitable tool to visualize AEA accumulation.

With this new tool, we provide evidence in favor of the existence of a specific mechanism for AEA internalization that is independent of FAAH activity.▊

REFERENCES

1. Di Marzo, V., L. De Petrocellis, F. Fezza, A. Ligresti, and T. Bisogno. 2002. Anandamide receptors. *Prostaglandins Leukot. Essent. Fatty Acids.* **66:** 377–391.

2. Howlett, A. C., F. Barth, T. I. Bonner, G. Cabral, P. Casellas, W. A. Devane, C. C. Felder, M. Herkenham, K. Mackie, B. R. Martin, et al. 2002. International Union of Pharmacology. XXVII. Classification of cannabinoid receptors. *Pharmacol. Rev.* **54:** 161–202.

3. Howlett, A. C., C. S. Breivogel, S. R. Childers, S. A. Deadwyler, R. E. Hampson, and L. J. Porrino. 2004. Cannabinoid physiology and pharmacology: 30 years of progress. *Neuropharmacology.* **47:** 345–358.

4. Egertova, M., B. F. Cravatt, and M. R. Elphick. 2003. Comparative analysis of fatty acid amide hydrolase and CB1 cannabinoid receptor expression in the mouse brain: evidence of a widespread role for fatty acid amide hydrolase in regulation of endocannabinoid signaling. *Neuroscience.* **119:** 481–496.

5. Maccarrone, M., L. De Petrocellis, M. Bari, F. Fezza, S. Salvati, V. Di Marzo, and A. Finazzi-Agrò. 2001. Lipopolysaccharide downregulates fatty acid amide hydrolase expression and increases anandamide levels in human peripheral lymphocytes. *Arch. Biochem. Biophys.* **393:** 321–328.

6. Nong, L., C. Newton, H. Friedman, and T. W. Klein. 2001. CB1 and CB2 receptor mRNA expression in human peripheral blood mononuclear cells (PBMC) from various donor types. *Adv. Exp. Med. Biol.* **493:** 229–233.

7. Klein, T. W., C. Newton, K. Larsen, L. Lu, I. Perkins, L. Nong, and H. Friedman. 2003. The cannabinoid system and immune modulation. *J. Leukoc. Biol.* **74:** 486–496.

8. Nunez, E., C. Benito, M. R. Pazos, A. Barbachano, O. Fajardo, S. Gonzalez, R. M. Tolon, and J. Romero. 2004. Cannabinoid CB2 receptors are expressed by perivascular microglial cells in the human brain: an immunohistochemical study. *Synapse.* **53:** 208–213.

9. Van Sickle, M. D., M. Duncan, P. J. Kingsley, A. Mouihate, P. Urbani, K. Mackie, N. Stella, A. Makriyannis, D. Piomelli, J. S. Davison, et al. 2005. Identification and functional characterization of brainstem cannabinoid CB2 receptors. *Science.* **310:** 329–332.

10. Fride, E. 2002. Endocannabinoids in the central nervous system—an overview. *Prostaglandins Leukot. Essent. Fatty Acids.* **66:** 221–233.

11. Parolaro, D., P. Massi, T. Rubino, and E. Monti. 2002. Endocannabinoids in the immune system and cancer. *Prostaglandins Leukot. Essent. Fatty Acids.* **66:** 319–332.

12. Battista, N., V. Gasperi, F. Fezza, and M. Maccarrone. 2005. The anandamide membrane transporter and the therapeutic implications of its inhibition. *Therapy.* **2:** 141–150.

13. Glaser, S. T., M. Kaczocha, and D. G. Deutsch. 2005. Anandamide transport: a critical review. *Life Sci.* **77:** 1584–1604.

14. Hillard, C. J., and A. Jarrahian. 2005. Accumulation of anandamide: evidence for cellular diversity. *Neuropharmacology.* **48:** 1072–1078.

15. McKinney, M. K., and B. F. Cravatt. 2005. Structure and function of fatty acid amide hydrolase. *Annu. Rev. Biochem.* **74:** 411–432.

16. Okamoto, Y., J. Morishita, K. Tsuboi, T. Tonai, and N. Ueda. 2004. Molecular characterization of a phospholipase D generating anandamide and its congeners. *J. Biol. Chem.* **279:** 5298–5305.

17. Fezza, F., V. Gasperi, C. Mazzei, and M. Maccarrone. 2005. Radiochromatographic assay of N-acyl-phosphatidylethanolamine-specific phospholipase D (NAPE-PLD) activity. *Anal. Biochem.* **339:** 113–120.

18. Liu, J., L. Wang, J. Harvey-White, D. Osei-Hyiaman, R. Razdan, Q. Gong, A. C. Chan, Z. Zhou, B. X. Huang, H. Y. Kim, et al. 2006. A biosynthetic pathway for anandamide. *Proc. Natl. Acad. Sci. USA.* **103:** 13345–13350.

19. Leung, D., A. Saghatelian, G. M. Simon, and B. F. Cravatt. 2006. Inactivation of N-acyl phosphatidylethanolamine phospholipase

D reveals multiple mechanisms for the biosynthesis of endocannabinoids. *Biochemistry.* **45:** 4720–4726.

20. Simon, G. M., and B. F. Cravatt. 2006. Endocannabinoid biosynthesis proceeding through glycerophospho-N-acyl ethanolamine and a role for alpha/beta-hydrolase 4 in this pathway. *J. Biol. Chem.* **281:** 26465–26472.

21. Piomelli, D., M. Beltramo, S. Glasnapp, S. Y. Lin, A. Goutopoulos, X. Q. Xie, and A. Makriyannis. 1999. Structural determinants for recognition and translocation by the anandamide transporter. *Proc. Natl. Acad. Sci. USA.* **96:** 5802–5807.

22. De Petrocellis, L., M. G. Cascio, and V. Di Marzo. 2004. The endocannabinoid system: a general view and latest additions. *Br. J. Pharmacol.* **141:** 765–774.

23. Van der Stelt, M., and V. Di Marzo. 2004. Endovanilloids. Putative endogenous ligands of transient receptor potential vanilloid 1 channels. *Eur. J. Biochem.* **271:** 1827–1834.

24. Sarker, K. P., and I. Maruyama. 2003. Anandamide induces cell death independently of cannabinoid receptors or vanilloid receptor 1: possible involvement of lipid rafts. *Cell. Mol. Life Sci.* **60:** 1200–1208.

25. Bari, M., N. Battista, F. Fezza, V. Gasperi, and M. Maccarrone. 2006. New insights into endocannabinoid degradation and its therapeutic potential. *Mini Rev. Med. Chem.* **6:** 109–120.

26. McFarland, M. J., and E. L. Barker. 2005. Anandamide transport. *Pharmacol. Ther.* **104:** 117–135.

27. Beltramo, M., N. Stella, A. Calignano, S. Y. Lin, A. Makriyannis, and D. Piomelli. 1997. Functional role of high-affinity anandamide transport, as revealed by selective inhibition. *Science.* **277:** 1094–1097.

28. Hillard, C. J., W. S. Edgemond, A. Jarrahian, and W. B. Campbell. 1997. Accumulation of N-arachidonoylethanolamine (anandamide) into cerebellar granule cells occurs via facilitated diffusion. *J. Neurochem.* **69:** 631–638.

29. Ortar, G., A. Ligresti, L. De Petrocellis, E. Morera, and V. Di Marzo. 2003. Novel selective and metabolically stable inhibitors of anandamide cellular uptake. *Biochem. Pharmacol.* **65:** 1473–1481.

30. Fegley, D., S. Kathuria, R. Mercier, C. Li, A. Goutopoulos, A. Makriyannis, and D. Piomelli. 2004. Anandamide transport is independent of fatty-acid amide hydrolase activity and is blocked by the hydrolysis-resistant inhibitor AM1172. *Proc. Natl. Acad. Sci. USA.* **101:** 8756–8761.

31. Ligresti, A., E. Morera, M. Van der Stelt, K. Monory, B. Lutz, G. Ortar, and V. Di Marzo. 2004. Further evidence for the existence of a specific process for the membrane transport of anandamide. *Biochem. J.* **380:** 265–272.

32. Oddi, S., M. Bari, N. Battista, D. Barsacchi, I. Cozzani, and M. Maccarrone. 2005. Confocal microscopy and biochemical analysis reveal spatial and functional separation between anandamide uptake and hydrolysis in human keratinocytes. *Cell. Mol. Life Sci.* **62:** 386–395.

33. Fowler, C. J. 2005. Pharmacological properties and therapeutic possibilities for drugs acting upon endocannabinoid receptors. *Curr. Drug Target. CNS Neurol. Disord.* **4:** 685–696.

34. Ligresti, A., M. G. Cascio, and V. Di Marzo. 2005. Endocannabinoid metabolic pathways and enzymes. *Curr. Drug Target. CNS Neurol. Disord.* **4:** 615–623.

35. Ortega-Gutierrez, S. 2005. Therapeutic perspectives of inhibitors of endocannabinoid degradation. *Curr. Drug Target. CNS Neurol. Disord.* **4:** 697–707.

36. Maccarrone, M., M. Di Rienzo, N. Battista, V. Gasperi, P. Guerrieri, A. Rossi, and A. Finazzi-Agrò. 2003. The endocannabinoid system in human keratinocytes. *J. Biol. Chem.* **278:** 33896–33903.

37. Maccarrone, M., F. Fezza, A. Finazzi-Agrò, and S. Oddi. 2006. Design and synthesis of biotinylated probes for N-acyl-ethanolamines. PCT/EP2006/061988. www.freepatentsonline.com/WO2007128344.html.

38. Maccarrone, M., M. Bari, and A. Finazzi-Agrò. 1999. A sensitive and specific radiochromatographic assay of fatty acid amide hydrolase activity. *Anal. Biochem.* **267:** 314–318.

39. Bari, M., A. Paradisi, N. Pasquariello, and M. Maccarrone. 2005. Cholesterol-dependent modulation of type 1 cannabinoid receptors in nerve cells. *J. Neurosci. Res.* **81:** 275–283.

40. Kathuria, S., S. Gaetani, D. Fegley, F. Valino, A. Duranti, A. Tontini, M. Mor, G. Tarzia, G. La Rana, A. Calignano, et al. 2003. Modulation of anxiety through blockade of anandamide hydrolysis. *Nat. Med.* **1:** 76–81.

41. Pertwee, R. G., and R. A. Ross. 2002. Cannabinoid receptors and their ligands. *Prostaglandins Leukot. Essent. Fatty Acids.* **66:** 101–121.

42. Muthian, S., K. Nithipatikom, W. B. Campbell, and C. J. Hillard. 2000. Synthesis and characterization of a fluorescent substrate for the N-arachidonoylethanolamine (anandamide) transmembrane carrier. *J. Pharmacol. Exp. Ther.* **293:** 289–295.

43. Di Marzo, V., A. Ligresti, E. Morera, M. Nalli, and G. Ortar. 2004. The anandamide membrane transporter. Structure-activity relationships of anandamide and oleoylethanolamine analogs with phenyl rings in the polar head group region. *Bioorg. Med. Chem.* **12:** 5161–5169.

44. Dainese, E., S. Oddi, M. Bari, and M. Maccarrone. 2007. Modulation of the endocannabinoid system by lipid rafts. *Curr. Med. Chem.* **14:** 2702–2715.

45. Szallasi, A., T. Szabo, T. Biro, S. Modarres, P. M. Blumberg, J. E. Krause, D. N. Cortright, and G. Appendino. 1999. Resiniferatoxin-type phorboid vanilloids display capsaicin-like selectivity at native vanilloid receptors on rat DRG neurons and at the cloned vanilloid receptor VR1. *Br. J. Pharmacol.* **128:** 428–434.

46. Maccarrone, M., M. Bari, T. Lorenzon, T. Bisogno, V. Di Marzo, and A. Finazzi-Agrò. 2000. Anandamide uptake by human endothelial cells and its regulation by nitric oxide. *J. Biol. Chem.* **275:** 13484–13492.

47. Ortega-Gutierrez, S., E. G. Hawkins, A. Viso, M. L. Lopez-Rodriguez, and B. F. Cravatt. 2004. Comparison of anandamide transport in FAAH wild-type and knockout neurons: evidence for contributions by both FAAH and the CB1 receptor to anandamide uptake. *Biochemistry.* **43:** 8184–8190.

48. McFarland, M. J., A. C. Porter, F. R. Rakhshan, D. S. Rawat, R. A. Gibbs, and E. L. Barker. 2004. A role for caveolae/lipid rafts in the uptake and recycling of the endogenous cannabinoid anandamide. *J. Biol. Chem.* **279:** 41991–41997.

49. Moore, S. A., G. G. Nomikos, A. K. Dickason-Chesterfield, D. A. Schober, J. M. Schaus, B. P. Ying, Y. C. Xu, L. Phebus, R. M. Simmons, D. Li, et al. 2005. Identification of a high-affinity binding site involved in the transport of endocannabinoids. *Proc. Natl. Acad. Sci. USA.* **102:** 17852–17857.

50. Alexander, J. P., and B. F. Cravatt. 2006. The putative endocannabinoid transport blocker LY2183240 is a potent inhibitor of FAAH and several other brain serine hydrolases. *J. Am. Chem. Soc.* **128:** 9699–9704.

51. Felder, C. C., A. K. Dickason-Chesterfield, and S. A. Moore. 2006. Cannabinoids biology: the search for new therapeutic targets. *Mol. Interv.* **6:** 149–161.

52. Di Marzo, V., M. Bifulco, and L. De Petrocellis. 2004. The endocannabinoid system and its therapeutic exploitation. *Nat. Rev. Drug Discov.* **3:** 771–784.